Adaptive Restoration of Speckled SAR Images*

José M. B. Dias, Tiago A. M. Silva, and José M. N. Leitão
Instituto Superior Técnico
Departamento de Engenharia Electrotécnica e de Computadores, and
Institttuo de Telecomunicações
Tel: +351 1 8418466; fax: +351 1 8418472; e-mail: bioucas@lx.it.pt

March 26, 1999

Abstract

The paper proposes a restoration method for speckled images generated by coherent imaging systems (e.g., synthetic aperture radar, synthetic aperture sonar, ultrasound imaging, and laser imaging). These systems are invariably affected by *speckle noise* and therefore restoration/filtering of the mean backsattered signal (*backsacttering coefficient*) is often necessary. The approach is Bayesian: the observed image is assumed to be a realization of a random field built upon the physical mechanism of image generation; the backscattering coefficient image is modelled by a *compound Gauss-Markov random field* which enforces smoothness on homogeneous regions while preserving discontinuities between neighboring regions. The *maximum a posteriori probability* (MAP) criterion is adopted. An *expectation maximization* type iterative scheme embeded in a a continuation algorithm is used to compute the MAP solution. Application examples performed on radar real and synthetic data are presented.

1 Introduction

Coherent imaging systems are designed aiming at the acquisition of the scene *complex reflectivity*. They are linear systems whose output is given by the convolution between its coherent *point spread function* (PSF) and the scene complex reflectivity. Examples are *synthetic aperture radar* (SAR), *synthetic aperture sonar* (SAS), *ultrasound imaging*, and laser imaging. The complex reflectivity originated in a given *resolution cell* is composed by the contributions of all individual scatterers lying in that cell. These contributions interfere randomly in a destructive or constructive manner, according to the spatial configuration of the scatterers. This random fluctuation is termed (*speckle noise*); its statistical properties has been addressed in several references [1], [2], [3]. Assuming that the surface being illuminated is rough compared to the wavelength, that there are no strong specular reflectors, and that there is a large number of scatterers per resolution cell, then the squared amplitude (*intensity*) of the complex reflectivity is exponentially distributed; the scenario just described, termed *fully developed speckle*, leads to highly noisy intensity images: the *signal to noise ratio* (SNR), defined as the square of the ratio between the intensity mean value (backscatering coefficient) and the intensity variance, is one. The granular appearance of intensity images is due to this very low SNR

Most applications involving coherent systems data rel
the mean intensity image (backscattering coefficient image
view of the rationale above presented, there is need for a
ing speckle reduction/restoration techniques to intensity da
common approach consists in averaging independent obs
tions of the same pixel, which in the case of SAR syste
called *multi-look*. This term stems from the fact that each
pendent sample is generated by a different segment of the
array. Independently of the system, an image formed by the
aging of m independent samples will herein be termed an m
image. For fully developed speckle, the SNR of an m-*loo*
age is m. However, increasing the number of independent
ples results in reduction of spatial resolution, being necessa
resort to spatial smoothing techniques. The basic idea und
ing these techniques is that of applying nonuniform smooth
in such a way that homogeneous image regions, in a stati
sense, are highly smooth, while discontinuities are preserve
[5], [6].

In recent years a significant research activity has been de
to the development of speckle reduction techniques, or, eq
lently, to the mean backscattering coefficient estimation. T
techniques take the form of image restoration [7], [8], edg
tection [9], or image segmentation algorithms [3], [10],
[12]. A common assumption is that images are locally sm
This behavior has been modeled mainly by *ad hoc* techni
[7], or by *Markov random fields* [3], [10], [11], [12].

The present approach is Bayesian:

- the observed image, given the backscattering coeffici
  is assumed to be a realization of a random field takin
  account the statistics of image reflectivity;

- the set of backscattering coefficients associated to th
  age pixels is assumed to be *piecewise smooth*, and
  elled as a random field with a *compound Gauss-M*
  random field (CGMRF) prior [5], [13].

The piecewise smoothness assumption makes sense in
situations: e.g., SAR images of agricultural landscapes, e
raphy of the human body, etc.

To our knowledge, modeling the backscattering coeffi
image with a CGMRF has not yet been addressed in the spe
image restoration context.

*This work was suppoted by Portuguese PRAXIS XXI program, under project 2/2.1.TIT/1580/95

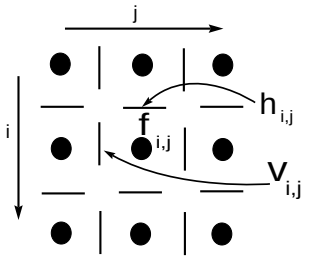

Figure 1: Relative positions of grids for the $\mathbf{f}$, $\mathbf{v}$, and $\mathbf{h}$ fields.

2 Proposed Approach

Assume that images are defined in the $N \times N$ rectangular lattice $Z_N = \{(i,j),\, i,j = 1,\ldots,N\}$. Define $\mathbf{F} = \{F_{ij}\}$ and $\mathbf{G} = \{G_{ij}\}$, with $(i,j) \in Z_N$ as the random fields associated to the backscattering coefficient image and the observed intensity image, respectively. Lowercase letters will denote the values assumed by the the random filds as well as its realizations. For compactness, the probability density of the generic field $\mathbf{X}$, $p_{\mathbf{x}}(\mathbf{X} = \mathbf{x})$, or of the generic random variable X, $p_x(X = x)$, will be denoted by $p(\mathbf{x})$ and p(x), respectively.

Besides fields $\mathbf{F}$ and $\mathbf{G}$, it is assumed the existence of another field, $\mathbf{L} = \{\mathbf{H}, \mathbf{V}\}$, with $\mathbf{H} = \{H_{ij}\}$ and $\mathbf{V} = \{V_{ij}\}$, signaling horizontal and vertical discontinuities. Variables V_{ij} and H_{ij} are binary, taking value 1 if a discontinuity is present and 0 otherwise. The field $\mathbf{L}$ also termed *line field* [5] serves the purpose of avoiding edges to be smoothed out during the restoration of field $\mathbf{F}$. Fig. 1 schematizes the spatial arrangement of $\mathbf{F}$ and $\mathbf{L}$.

The present work aims at the estimation of the backscattering coefficient, $\mathbf{F}$, and the line field, $\mathbf{L}$, from the observed image $\mathbf{G}$. Since our approach is Bayesian it is model-based, therefore not only the the image generation mechanism $p(\mathbf{g}|\mathbf{f},\mathbf{l})$, but also the prior density $p(\mathbf{f},\mathbf{l})$, which captures the model, must be specified.

2.1 Image Generation Mechanism

Under the fully developed speckle hypothesis, the complex amplitude $x = x_r + jx_i$ (inphase and quadrature components) of the backscattered field, at each pixel, is circularly symmetric and Gaussian [10]. Thus

$$p(x|f) = \frac{1}{\pi f^2} e^{-\frac{|x|^2}{f^2}}, \tag{1}$$

where $f^2 := E[|x|^2]$ is the backscattering coefficient of the referred resolution cell. For intensity or power images the data is in the form of square magnitude of the complex components, $g = |x_r + jx_i|^2$. Random variable G is therefore the exponentially distributed:

$$p(g|f) = \frac{1}{f^2} e^{-\frac{g}{f^2}}. \tag{2}$$

For an m-look image, G is the average of m independent exponentially distributed random variables, thus having a gamma density [14],

$$p(g|f) = \frac{1}{\Gamma(M)} \left(\frac{f^2}{M}\right)^{-M} g^{M-1} \exp\left(-\frac{gM}{f^2}\right),$$

with $E[g|f] = f^2$ and $\sigma^2\,[g|f] = f^4/M$.

It is herein assumed that the components of $\mathbf{g}$ given $\mathbf{f}$ ar dependent. Hence

$$p(\mathbf{g}|\mathbf{f}) = \prod_{ij \in Z_N} p(g_{ij}|f_{ij}).$$

The conditional independence assumption is valid if the re tion cells associated to any pair of pixels are disjoint. Th only true if the size of the imaging system PSF is smaller the corresponding interpixel distance. This is approximately in most acquisition systems. Otherwise, neighboring data w be extremely correlated adding no information.

2.2 Prior Model

Image $\mathbf{f}$ is assumed to be *piecewise smooth*. This makes s whenever the scene is made of smooth regions, concernin backscattering coefficient. *Gauss-Markov random fields* [15 both mathematically and computationally suitable for repre ing local interactions, and particularly continuity between n boring pixels. However, the continuity constraint must be carded for those pixels near the discontinuities. For this pur we take the *first order* noncausal CGMRF

$$p(\mathbf{f}|\boldsymbol{l}) \propto \exp\left\{-\frac{\mu}{2}\sum_{ij}(\Delta^h_{ij})^2\bar{v}_{ij} + (\Delta^v_{ij})^2\bar{h}_{ij}\right\},$$

where $\bar{v}_{ij} := (1 - v_{ij})$, $\bar{h}_{ij} := (1 - h_{ij})$, $\Delta^h_{ij} := (f_{ij} - f_{i,}$ $\Delta^v_{ij} := (f_{ij} - f_{i-1,j})$, and μ^{-1} has the meaning of the var of the increments Δ^h_{ij} and Δ^v_{ij}. Notice that continuity cons between pixels (i,j) and $(i,j-1)$ is removed if variable v_{ij} to one; the same is true concerning horizontal lines. Mode is not, however, normalizable and therefore it is not a probal density function. To solve this problem, the following prior proposed in [13]:

$$p(\mathbf{f}|\boldsymbol{l}) = \frac{1}{Z(\mathbf{l})} e^{-\frac{\mu}{2}\sum_{ij}\omega(\Delta^h_{ij})^2\bar{v}_{ij} + \omega(\Delta^v_{ij})^2\bar{h}_{ij} + (1-4\omega))f^2_{ij}}$$

where ω is the discontinuity smoothness parameter, w should be chosen so as to $\omega < 1/4$, and $Z(\mathbf{l})$ is a normal constant depending on $\mathbf{l}$, termed *partition function*. For v of ω very close to $1/4$ the third term of (6) affects very litt result, yet leads to an integrable prior $p(\boldsymbol{f}|\boldsymbol{l})$.

Apart a constant, the inverse of the partition function is given by the determinant of the $N^2 \times N^2$-matrix assoc to the quadratic form present in (6). This is an unbearable due to the typically huge size of the matrix involved and due to its irregularity associated to the particular disconti pattern. To circumvent the difficulty therein, the density p is replaced by the Besag's pseudolikelihood approxim

[15]. Definig $f_{N_{ij}} := \{f_{i,j-1}, f_{i,j+1}, f_{i-1,j}, f_{i+1,j}\}$, $l_{N_{ij}} := \{h_{i,j}, v_{i,j}, h_{i+1,j}, v_{i,j+1}\}$, $\bar{f}_{ij} := \bar{h}_{ij} f_{i-1,j} + \bar{h}_{i+1,j} f_{i+1,j} + \bar{v}_{ij} f_{i,j-1} + \bar{v}_{i,j+1} f_{i,j+1}$, and

$$\eta_{ij} := \lambda_{ij}^2 \mu \omega \bar{f}_{ij} \quad (7)$$

$$\lambda_{ij}^2 := \frac{1}{\mu[1 - \omega(v_{ij} + v_{i,j+1} + h_{ij} + h_{i+1,j})]}, \quad (8)$$

the pseudolikelihood approximation is written as (see [16])

$$p(\boldsymbol{f}|\mathbf{l}) \simeq \prod_{ij} p(f_{i,j}|f_{N_{i,j}}, l_{N_{i,j}})$$

$$= \prod_{ij} \frac{1}{\sqrt{2\pi}\lambda_{ij}} \exp\left\{-\frac{1}{2\lambda_{ij}^2}(f_{ij} - \eta_{ij})^2\right\} \quad (9)$$

$$= \frac{e^{-\mu \sum_{ij} \omega(\Delta_{ij}^h)^2 \bar{v}_{ij} + \omega(\Delta_{ij}^v)^2 \bar{h}_{ij} + \frac{1}{2}(1-4\omega)) f_{ij}^2}}{\prod_{ij} \sqrt{2\pi}\lambda_{ij}} \quad (10)$$

where expression (10) is obtained from (9) after a simple but lengthy manipulation.

The probability $p(\mathbf{l})$ is chosen, as in the *weak membrane* [4] model, to add a penalty to each discontinuity signaled:

$$p(l) = \frac{1}{Z_\alpha} e^{-\alpha ||l||}, \qquad \alpha > 0, \quad (11)$$

where $||l|| := \sum_{ij}(v_{ij} + h_{ij})$. Prior (11) is only a function of the number of discontinuities signaled.

2.3 Joint Density

Invoking the Bayes rule, and noting that $p(\mathbf{g}|\mathbf{f}, \mathbf{l}) = p(\mathbf{g}|\mathbf{f})$, we obtain the joint probability density function of $(\mathbf{f}, \mathbf{l}, \mathbf{g})$ as

$$p(\mathbf{f}, \mathbf{l}, \mathbf{g}) = p(\mathbf{g}|\mathbf{f}) p(\mathbf{f}|\mathbf{l}) p(\mathbf{l}). \quad (12)$$

Replacing expressions (3), (10), and (11) in (12), the joint distribution of $\mathbf{f}, \mathbf{l}$ conditioned on $\mathbf{g}$, is then given by

$$p(\mathbf{f}, \mathbf{l}|\mathbf{g}) = \frac{1}{Z} e^{-U(\mathbf{f}, \mathbf{l}|\mathbf{g})}, \quad (13)$$

where

$$-U(\mathbf{f}, \mathbf{l}|\mathbf{g}) = \quad (14)$$

$$- \quad 2M \log f_{ij} - \frac{M g_{ij}}{f_{ij}^2}$$

$$- \quad \mu \sum_{ij} \omega \bar{v}_{ij} (\Delta_{ij}^h)^2 + \omega \bar{h}_{ij} (\Delta_{ij}^v)^2 + \frac{1}{2}(1 - 4\omega) f_{ij}^2$$

$$- \quad \sum_{ij} \log \lambda_{ij} - \log Z_\alpha - \alpha ||l|| + c^{te}. \quad (15)$$

3 Computing the MAP solution

The *maximum a posteriori probability* (MAP) criterion is adopted for estimating both $\boldsymbol{f}$ and $\boldsymbol{l}$. Accordingly

$$(\widehat{\mathbf{f}}, \widehat{\mathbf{l}})_{MAP} = \arg\max_{\mathbf{f}, \mathbf{l}} p(\mathbf{f}, \mathbf{l}|\mathbf{g}). \quad (16)$$

Computing the MAP solution leads to a huge non-conve
timization problem, involving continous and discrete varia
with unbearable computation burden. Instead of determinin
actly $(\widehat{\mathbf{f}}, \widehat{\mathbf{l}})_{MAP}$, we propose a continuation method whic
though not yielding the global maximum of $p(\mathbf{f}, \mathbf{l}|\mathbf{g})$, del
nearly optimum estimates with a feasible computational
Aiming at this goal, define

$$p(\mathbf{f}, \mathbf{l}|\mathbf{g}, \beta) = \frac{1}{Z(\beta)} e^{-\beta U(\mathbf{f}, \mathbf{l}|\mathbf{g})}.$$

Under a statistical physical interpretation, parameter β i
inverse of the temperature ($\beta = 1/T$); this parameter cor
the prominence of the maxima of (17): when $\beta \to 0$, all co
urations of $(\mathbf{f}, \mathbf{l})$ are equiproblable; when $\beta \to \infty$, the abs
maxima becomes progressively more marked, and in limi
set of the absolute maxima have probability one.

Annealing algorithms, be it stochastic or deterministic
ploit this behaviour to establish continuation methods in w
the temperature plays the role of continuation parameter.

The proposed continuation scheme evaluates, for an inc
ing sequence β_t, with $t = 1, \ldots, t_m$, the maximum $\widehat{\mathbf{f}}^{(t)}$
$p(\mathbf{f}, \widehat{\mathbf{l}}^{(t-1)}|\mathbf{g})$, with respect to $\mathbf{f}$, follwed by the *mean line*
$\widehat{\mathbf{l}}^{(t)} = E_{\beta_t}[\mathbf{l}|\widehat{\mathbf{f}}^{(t)}, \mathbf{g}]$ (symbol E_β denotes the mean value
ator computed according to density (17)). Based on this o
tion the algorithm is termed *expectation maximization anne*
(EMA).

EMA Algorithm

Initialization: set $\widehat{h}_{ij}^{(0)} = \widehat{v}_{ij}^{(0)} := 0.5$, $t = 1$, β_0, a, m
DO

step 1: $\widehat{\mathbf{f}}^{(t)} = \arg\max_{\mathbf{f}} p(\mathbf{f}, \widehat{\mathbf{l}}^{(t-1)}|\mathbf{g})$ (18)

step 2: $\widehat{\mathbf{l}}^{(t)} = E_{\beta_t}[\mathbf{l}|\widehat{\mathbf{f}}^{(t)}, \mathbf{g}]$ (19)

step 3: $\beta_{t+1} = a\beta_t$ (20)

While $t \leq m$

Due to the the already pointed out behaviour of (17), it fol
that

$$E_\beta[\mathbf{l}|\mathbf{f}, \mathbf{g}] \to \arg\max_{\mathbf{l}} p(\mathbf{f}, \mathbf{l}|\mathbf{g}), \qquad \beta \to \infty.$$

Therefore the stationaty points of the EMA algorithm ar
least, local maxima of $p(\mathbf{f}, \mathbf{l}|\mathbf{g})$; the *quality* of the maxim
pends on the schedule of β_t.

Maximization (18) is implemented by the *iterated condit
modes* (ICM) method [15]. This is an coordinate-wise a
technique, that maximizes the posterior distribution with re
to each individual component. After sweeping all image
procedure is repeated until no noticiable energy increment
obtained.

The sationary points of (15), with respect to f_{ij}, are zer
the fourth order polynomial

$$-\mu\left((1 - 4\omega) + 2\omega(\bar{h}_{ij} + \bar{h}_{i+1,j} + \bar{v}_{ij} + \bar{v}_{i,j+1})\right) f_{ij}^4$$

$$+2\mu\omega\bar{f}_{ij}f_{ij}^3 - 2Mf_{ij} + 2Mg_{ij} = 0. \quad (22)$$

For each pixel (i,j) the solution of equation (22) is chosen to be the one root that maximizes $p(\mathbf{f}, \widehat{\mathbf{l}}^{(t-1)}|\mathbf{g})$.

Step (19) of the EMA algorithm is similar to the equivalent step of *mean field algoritm* (MFA); using the rationale proposed in [6], one obtains

$$v_{ij} := E_\beta[v_{ij}|\mathbf{f},\mathbf{g}] \quad \simeq \quad \frac{1}{1+e^{\beta\left\{\alpha_{ij}^v - \mu\omega(\Delta_{i,j}^h)^2\right\}}}, \quad (23)$$

where $\alpha_{ij}^v = \alpha + \frac{1}{2}\log t_{ij}^v$ and (see [16])

$$\begin{aligned} t_{ij}^v \quad &= \quad \frac{[1-\omega(v_{i,j-1}+h_{i,j-1}+h_{i+1,j-1})]}{[1-\omega(1+v_{i,j-1}+h_{i,j-1}+h_{i+1,j-1})]} \\ &\times \quad \frac{[1-\omega(v_{i,j+1}+h_{ij}+h_{i+1,j})]}{[1-\omega(1+v_{i,j+1}+h_{ij}+h_{i+1,j})]}. \end{aligned} \quad (24)$$

A similar result is obtained for $\bar{h}_{ij} := E_\beta[h_{ij}|\mathbf{f},\mathbf{g}]$, replacing h by v and vice versa (23) and (24).

The EMA algorithm differs from the MFA one in the step (19): while the latter evaluates mean value $E_{\beta_t}[\mathbf{f}|\widehat{\mathbf{l}}^{(t)},\mathbf{g}]$, the former maximizes $p(\mathbf{f},\widehat{\mathbf{l}}^{(t)}|\mathbf{g})$ with respect to $\mathbf{f}$. For Gaussian observation models both estimates are equal. This is not, however, the present case, since the obsevation model is not Gaussian.

Although not explicitly, function $p(\mathbf{f},\mathbf{l}|\mathbf{g})$ depends on parameters μ and α. The maximum likelihood estimate of μ is

$$\widehat{\mu}_{ML} = \frac{N^2}{2\sum_{ij}\omega\bar{v}_{ij}(\Delta_{ij}^h)^2 + \omega\bar{h}_{ij}(\Delta_{ij}^v)^2 + \frac{1}{2}(1-4\omega)f_{ij}^2}. \quad (25)$$

Therefore, if μ is unknown, it can be iteratively evaluated when implementing the EMA.

The setting of parameter α, depends on the tresholding above which discontinuities are signaled. This can be understood from expression (23), which for hight values of β leads to the following decision rule:

$$v_{ij} = \begin{cases} 1, & (f_{ij}-f_{i,j-1})^2 > \frac{\alpha+\frac{1}{2}\log t_{ij}^v}{\mu\omega} \\ 0, & (f_{ij}-f_{i,j-1})^2 < \frac{\alpha+\frac{1}{2}\log t_{ij}^v}{\mu\omega}. \end{cases} \quad (26)$$

Assume that the discontinuities from which t_{ij} depends are all set to zero. In this case we have $\frac{1}{2}\log t_{ij}^v = 0.29$, which tipically verifies $\alpha \gg \log t_{ij}^v$; a vertical discontinuity is therefore signaled if $\Delta_{ij}^h > \sqrt{\alpha/(\mu\omega)}$. If some discontinuities from which t_{ij} depends are set to one, the treshold $\frac{\alpha+\frac{1}{2}\log t_{ij}^v}{\mu\omega}$ increases, preventing an over segmented image, namely the creation of double edges.

4 Experimental Results

In this section we present restoration results applied to synthetic and real data. The EMA algoritm is parametrized with $m = 10$ (number of iterations), and $a = 1.259$ (increasing rate of β). Parameter μ is estimated according to (25).

Fig. 2 shows a restoration example of a synthetic image. The different image parts show:

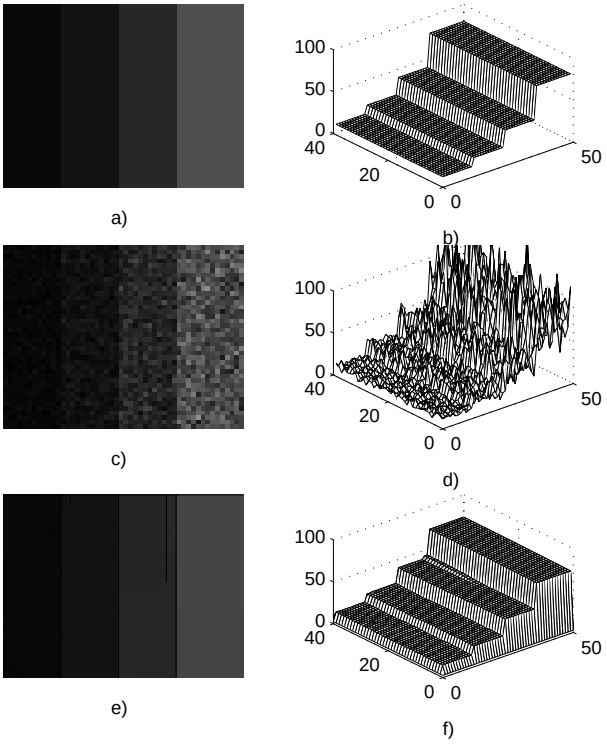

Figure 2: Synthetic image: a) and b) original image; c) a square root of noisy images generated for 3-looks; e) and stored image. In e) the resulting segmentation is superimpo

(a,b) the original parameter image comprising 4 constar gions;

(c,d) square root of the gamma image generated using the vious image as parameter with $M = 3$ (number of lo

(e,f) the restored image.

Both images are showed as colormaps and surfaces for b perception. In the estimated image, the estimated discontinu are overimposed. The estimated image exhibits nearly perf preserved edges. Within each region the image is smooth a original image and the estimated values are very close t original. Although the estimation was based on a very noisy age (*signal-to-noise ratio* of 4.7 dB) the results were expec due to the fact that the image complies totaly with the CG prior.

Fig. 3(a) shows a SAR image of the agricultural landsca Flevoland region in northern Netherlands. The image was tured in Radarsat's standard mode (pixel spacing $\simeq$ 12.5m has four-looks. Part (b) displays the restored image with the field superimposed. The EMA algorithm performs very we it can be perceived from the plot shown in part (c) of Fig the squared root of intensity data jointly with the restored age are plotted for column 300 (image has size 512×512) algorithm correctly smooth data within homogeneous reg preserving discontinuities between neighboring regions.

a)

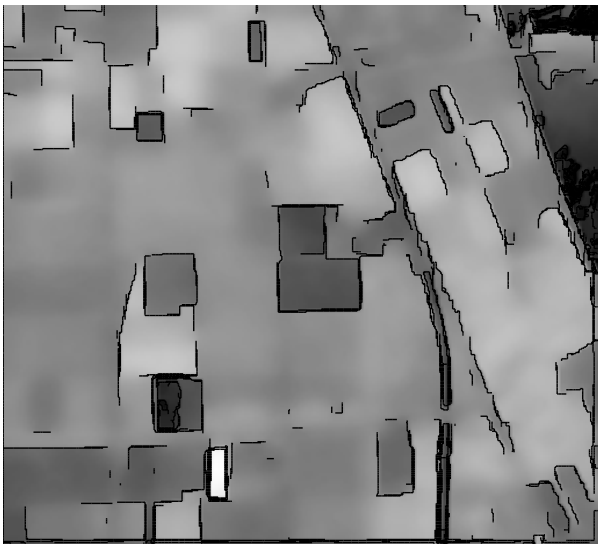

b)

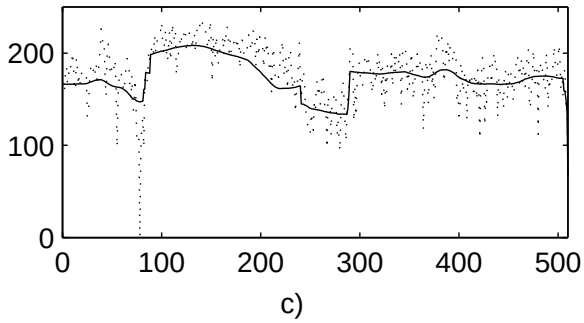

c)

Figure 3: Radarsat SAR image of agricultural fields in the Flevoland, Netherlands: a) original image; b) estimated image considering $M = 4$. The resulting segmentation is superimposed on both a) and b); estimated values along a straight line.

5 Concluding Remarks

A new method for edge-preserving restoration of coheren ages was presented. The knowledge of the statistics of the sp led images was fully taken into account through the observ model. The prior, a *compund Gauss Markov random field* used to tackle images exhibiting piecewise homogenous reg

Restoration examples, comprising very noisy synthetic SAR images, suggest the adequacy of the proposed meth ogy. Estimation of the model's parameters, will be furthe proved in order to render the algorithm more robust and matic.

References

[1] S. Lowenthal and H. Arsenault, "Image formation for col diffuse objects: statistical properties", *J. Opt. Soc. Amer.*, vo pp. 1487–1493, Nov. 1970.

[2] J. Goodman, "Some fundamental properties of speckle", *J Soc. Amer.*, vol. 66, pp. 1145–1150, Nov. 1976.

[3] H. Derin, P. Kelly, G. Vézina, and S. Labitt, "Modelling an mentation of speckled images using complex data", *IEEE Geosci. Remote Sensing*, vol. 28, pp. 76–87, 1990.

[4] A. Blake and A. Zisserman, *Visual Reconstruction*, MIT Cambridge, M.A., 1987.

[5] S. Geman and D. Geman, "Stochastic relaxation, Gibbs dis tion and the Bayesian restoration of images", *IEEE Trans. P Analysis and Machine Intelligence*, vol. PAMI-6, pp. 721 Nov. 1984.

[6] D. Geiger and F. Girosi, "Parallel and deterministic algor from MRF's: Surface reconstruction", *IEEE Trans. Pattern ysis and Machine Intelligence*, vol. PAMI-13, pp. 401–412 1991.

[7] V. Frost, K. Shanmugan, and J. Holtzman, "A model for images and its applications to adaptive digital filtering of plicative noise", *IEEE Trans. on Pattern Analysis and Ma Intelligence*, vol. 2, pp. 157–166, 1982.

[8] D. Kuan, A. Sawchuk, T. Strand, and P. Chavel, "Adaptive re tion of images with speckle", *IEEE Trans. Acoust. Speech Process.*, vol. 35, pp. 373–383, 1987.

[9] A. Bovik, "On detecting edges in speckle imagery", *IEEE Acoust. Speech Signal Process.*, vol. 36, pp. 1618–1627, 19

[10] P. Kelly, H. Derin, and K. Hartt, "Adaptive segmentation of s led images using a hierarchical random field model", *IEEE Acoust. Speech Signal Process.*, vol. 38, pp. 1628–1641, 19

[11] E. Rignot and R. Chellapa, "Segmentation of polarimetri thetic aperture radar data", *IEEE Trans. Image Process.*, v pp. 281–300, 1992.

[12] A. Solberg, Torfinn Taxt, and A. Jain, "A Markov random model for classification of multisource satellite imagery", *Trans. Geosci. Remote Sensing*, vol. 34, pp. 100–113, 1996.

[13] F. Jeng and J. Woods, "Compound Gauss-Markov random for image processing", in A.Katsaggelos, editor, *Digital Restoration*, pp. 89–108. Springer Verlag, 1991.

[14] R. Touzi, A. Lopes, and P. Bousquet, "A statistical and ge rical edge detector for sar images", *IEEE Trans. Geosci. R Sensing*, vol. 26, pp. 764–773, 1988.

[15] J. Besag, “On the statistical analysis of dirty pictures”, *Journal of the Royal Statistical Society B*, vol. 48, pp. 259–302, 1986.

[16] M. Figueiredo and L. Leitão, “Unsupervised image restoration and edge location using compound Gauss-Markov random fiels and the MDL principle”, *IEEE Trans. Image Processing*, vol. 6, pp. 1089–1102, August 1997.